Characteristics of Coplanar Transmission Lines on Multilayer Substrates: Modeling and Experiments

Erli Chen and Stephen Y. Chou, *Senior Member, IEEE*

***Abstract*— Characteristics of coplanar transmission lines on multilayer substrates expressed in analytic formulas have been obtained using conformal mapping. The accuracy of these formulas has been verified experimentally on a variety of coplanar transmission lines using differential electro-optic (DEOS) sampling. For coplanar waveguides, the theory differs from the experiment by less than 3%; for coplanar striplines, the differences are less than 6%.**

I. Introduction

TODAY'S HIGH-speed electronic devices can successfully operate at frequencies far above 100 GHz [1]–[3]. At such high frequencies, transmission lines have to be used for device connection and signal distribution to retain the signal fidelity. Among all the choices of transmission lines, coplanar transmission lines (CTL's), including coplanar waveguides (CPW's) and coplanar striplines (CPS's), have attracted the most attention owing to their integration capability with electronic devices and fabrication compatibility with modern ultra-large-scale integration (ULSI) processing. In addition, CTL's are important components in the ultrafast signal characterization [4], [5] and monolithic microwave integrated circuits [6]–[8].

Theoretical studies of transmission lines are carried out typically by either full-wave or quasi-static analysis [9]. Since full-wave analysis requires time-consuming numerical calculations, quasi-static analysis, which provides analytic formulas, is generally preferred in transmission-line design. The first analytic formulas for calculating quasi-static wave parameters of CPW's have been given by Wen, obtained using conformal mapping [10]. However, Wen's formulas are based on the assumption that the substrate thickness is infinitely large and the ground wires of the CPW's are infinitely wide [11], [12]. Veyres and Fouad Hanna have extended the application of conformal mapping to CPW's with finite dimensions and substrate thicknesses [13]. Their formulas have been proven experimentally to be quite accurate by several authors [13], [14]. Fouad Hanna also has derived analytic formulas for CPS's on substrates with finite thicknesses [15]. His results, however, have a good accuracy only if the thicknesses of substrates are larger than the line dimensions, but diverge otherwise. To solve this problem, Ghione *et al.* have obtained more generalized formulas using the duality principle that the phase velocities of complementary lines are equal [14].

Manuscript received August 7, 1996; revised February 28, 1997.

E. Chen is with Seagate Technology, Minneapolis, MN 55435 USA.

S. Y. Chou is with the Nano Structure Laboratory, Department of Electrical Engineering, University of Minnesota, Minneapolis, MN 55455 USA.

Publisher Item Identifier S 0018-9480(97)03917-3.

However, all these analytic formulas are useful only for the transmission lines on substrates with a single dielectric layer. In practice, there are many circumstances in which the substrates are multilayer. For example, in integrated circuits, connection lines are either on or buried between dielectric layers. To date, only full-wave analyses on multilayer substrates have been reported [16]–[18]. In this paper, conformal mapping is used to derive the analytic formulas for CPW's and CPS's on multilayer substrates. The accuracy of these formulas is then verified experimentally on a variety of CTL's using differential electro-optic (EO) sampling (DEOS).

II. Theory

In this section, conformal mapping is applied to obtain the characteristics of CPW and CPS transmission lines in the form of analytic formulas. The validity of conformal mapping in transmission-line analysis fully relies on the assumption that the propagation mode in the transmission lines is quasi-static, i.e., it is a pure TEM mode. As pointed out before, quasi-static approximation is valid up to a frequency of 100 GHz [18]. Moreover, frequency-dependent (nonquasi-static) formulas can be obtained easily by modifying the quasi-static formulas [19]–[21].

Using the quasi-static approximation, the effective dielectric constant $\epsilon_{\rm eff}$, phase velocity $\nu_{\rm ph}$, and characteristic impedance, Z_0, of a transmission line are given as [9]

$$\epsilon_{\rm eff} = \frac{C}{C_0} \tag{1}$$

$$\nu_{\rm ph} = \frac{c}{\sqrt{\epsilon_{\rm eff}}} \tag{2}$$

$$Z_0 = \frac{1}{C\nu_{\rm ph}} \tag{3}$$

where c is the speed of light in free space, C is the line capacitance of the transmission line, and C_0 is the line capacitance of the transmission line when no dielectrics exist. Therefore, in order to obtain the quasi-static wave parameters of a transmission line, we only have to find the capacitances C and C_0.

The configurations of the CTL's used for the analysis are shown in Fig. 1(a) and 1(b), i.e., CPW and CPS transmission lines sandwiched between two top and three bottom dielectric layers. The concepts developed in this section, however, are not limited to these structures—more layers can be added. In the following analysis, we assume that the transmission lines are infinite thin and the dielectrics are infinite wide. Correc-

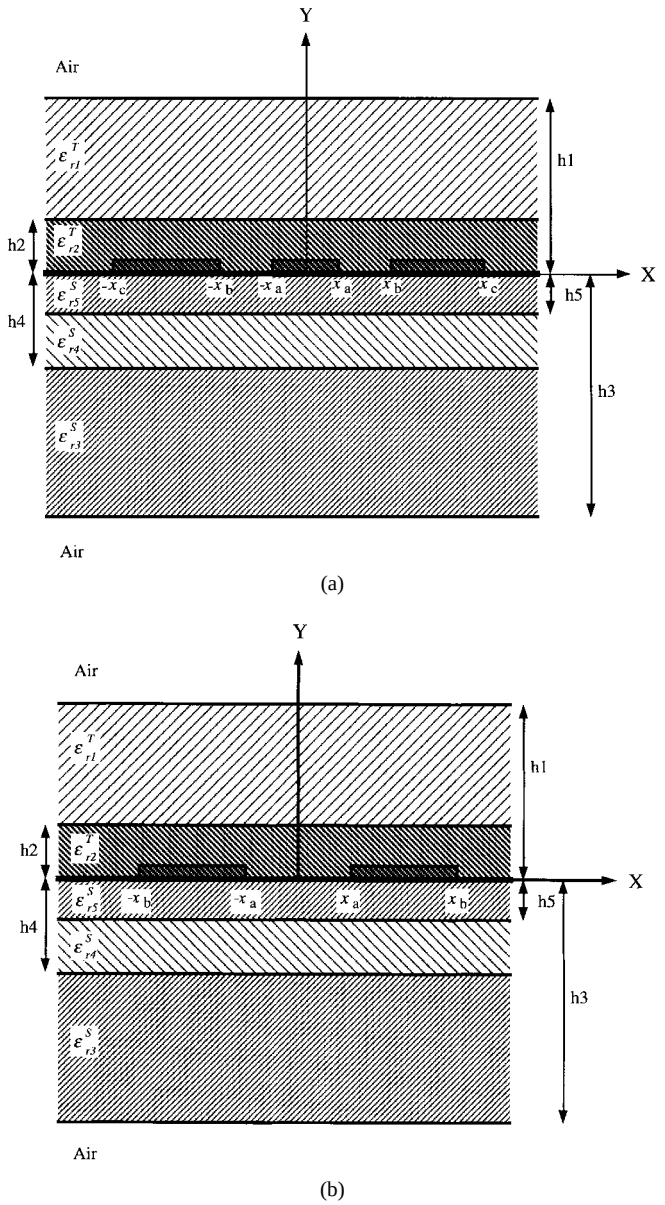

Fig. 1. Configurations of the (a) CPW and (b) CPS transmission lines used for the analysis. The superscript letter "T" on the dielectric constant stands for the top dielectrics, and the subscript letter "S" stands for substrate dielectrics.

tions can be made when the thicknesses of the transmission lines and widths of the dielectrics are finite [9], [22].

A. Wave Parameters of CPW's

The Veyers–Fouad Hanna approximation (superposition of partial capacitances) [13] is extended to our case, in which the line capacitance of the CPW shown in Fig. 1(a) can be written as the sum of six line capacitances, i.e.,

$$C_{\mathrm{CPW}} = C_0 + C_1 + C_2 + C_3 + C_4 + C_5. \tag{4}$$

The configurations of these capacitances are shown in Fig. 2(a)–(f). We will discuss the definition of each capacitance in more detail later. The capacitance calculated using the method of superposition of partial capacitances is exact when all the boundaries of the dielectrics are along the electric field lines. In this case, magnetic walls can be placed along the dielectric boundaries, and the capacitance of a transmission line can be divided into partial capacitances without affecting the field [22]. In a CTL on a multilayer substrate, however, the dielectric boundaries are not along the field lines, and the accuracy in application of the superposition of partial capacitance has to be verified experimentally. Although Veyers–Fouad Hanna's approximation has been proven to be quite accurate for the transmission lines on single-dielectric-layer substrates [13], [18], its accuracy for multilayer substrates is still unknown, and will be the subject of Sections III and IV.

1) Calculation of C_0: As shown in Fig. 2(a), C_0 is the line capacitance of the CPW in the absence of all dielectrics. This boundary problem can be solved using conformal mapping [13], which gives

$$C_0 = 4\epsilon_0 \frac{K'(k)}{K(k)} \tag{5}$$

where K is the complete elliptical integral of the first kind, and $K'(k) = K(k')$. The variables k and k' are geometrically dependent, and are given as

$$k = \frac{x_c}{x_b}\sqrt{\frac{x_b^2 - x_a^2}{x_c^2 - x_a^2}} \tag{6a}$$

$$k' = \sqrt{1 - k^2}. \tag{6b}$$

2) Calculation of C_2: The configuration of C_1 is shown in Fig. 2(b), in which the electrical field exists only in a dielectric layer with thickness of h_1 and relative dielectric constant of $\epsilon_{r1}^T - 1$. Using conformal mapping [13], we have

$$C_1 = 2\epsilon_0(\epsilon_{r1}^T - 1)\frac{K'(k_1)}{K(k_1)} \tag{7}$$

where

$$k_1 = \frac{\sinh\left(\frac{\pi x_c}{2h_1}\right)}{\sinh\left(\frac{\pi x_b}{2h_1}\right)}\sqrt{\frac{\sinh^2\left(\frac{\pi x_b}{2h_1}\right) - \sinh^2\left(\frac{\pi x_a}{2h_1}\right)}{\sinh^2\left(\frac{\pi x_c}{2h_1}\right) - \sinh^2\left(\frac{\pi x_a}{2h_1}\right)}} \tag{8a}$$

$$k_1' = \sqrt{1 - k_1^2}. \tag{8b}$$

3) Calculation of C_2, C_3, C_4, and C_5: C_2, C_3, C_4, and C_5 are, respectively, the line capacitances when the electric field exists only inside the dielectric layers with thicknesses of h_2, h_3, h_4, and h_5, and relative dielectric constants of $\epsilon_{r2}^T - \epsilon_{r1}^T$, $\epsilon_{r3}^S - 1$, ϵ_{r3}^S, and $\epsilon_{r5}^S - \epsilon_{r4}^S$ [Fig. 2 (c)–(f)]. Using the method demonstrated in Section II, we obtain

$$C_2 = 2\epsilon_0(\epsilon_{r2}^T - \epsilon_{r1}^T)\frac{K'(k_2)}{K(k_2)} \tag{9}$$

$$C_3 = 2\epsilon_0(\epsilon_{r3}^S - 1)\frac{K'(k_3)}{K(k_3)} \tag{10}$$

$$C_4 = 2\epsilon_0(\epsilon_{r4}^S - \epsilon_{r3}^S)\frac{K'(k_4)}{K(k_4)} \tag{11}$$

$$C_5 = 2\epsilon_0(\epsilon_{r5}^S - \epsilon_{r4}^S)\frac{K'(k_5)}{K(k_5)} \tag{12}$$

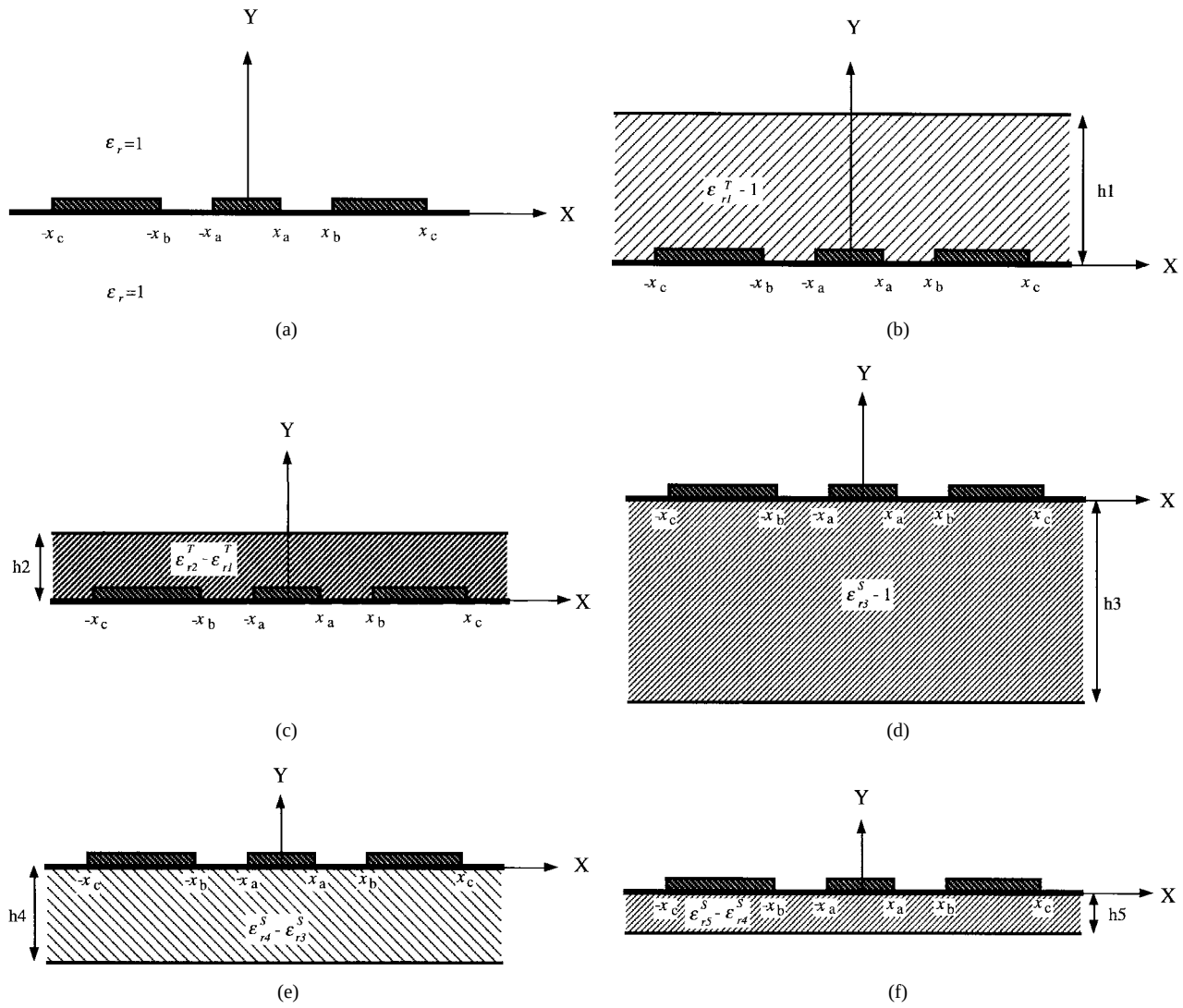

Fig. 2. Configurations of capacitances (a) C_0, (b) C_1, (c) C_2, (d) C_3, (e) C_4, and (f) C_5.

where

$$k_i = \frac{\sinh\left(\frac{\pi x_c}{2h_i}\right)}{\sinh\left(\frac{\pi x_b}{2h_i}\right)} \sqrt{\frac{\sinh^2\left(\frac{\pi x_b}{2h_i}\right) - \sinh^2\left(\frac{\pi x_a}{2h_i}\right)}{\sinh^2\left(\frac{\pi x_c}{2h_i}\right) - \sinh^2\left(\frac{\pi x_a}{2h_i}\right)}} \tag{13a}$$

$$k_i' = \sqrt{1 - k_i^2}. \tag{13b}$$

4) Calculation of $\epsilon_{\text{eff}}^{\text{CPW}}$, $v_{\text{ph}}^{\text{CPW}}$, and Z_0^{CPW}: Substituting (4), (5), (7), and (9)–(12) into (1) results in

$$\begin{aligned}\epsilon_{\text{eff}}^{\text{CPW}} &= \frac{C_{\text{CPW}}}{C_0} \\ &= 1 + \frac{1}{2}(\epsilon_{r1}^T - 1)\frac{K(k)K(k_1')}{K(k')K(k_1)} \\ &\quad + \frac{1}{2}(\epsilon_{r2}^T - \epsilon_{r1}^T)\frac{K(k)K(k_2')}{K(k')K(k_2)} \\ &\quad + \frac{1}{2}(\epsilon_{r3}^S - 1)\frac{K(k)K(k_3')}{K(k')K(k_3)} \\ &\quad + \frac{1}{2}(\epsilon_{r4}^S - \epsilon_{r3}^S)\frac{K(k)K(k_4')}{K(k')K(k_4)} \\ &\quad + \frac{1}{2}(\epsilon_{r5}^S - \epsilon_{r4}^S)\frac{K(k)K(k_5')}{K(k')K(k_5)}.\end{aligned} \tag{14}$$

Using (2) and (3), we have

$$\nu_{\text{ph}}^{\text{CPW}} = \frac{c}{\sqrt{\epsilon_{\text{eff}}^{\text{CPW}}}} \tag{15}$$

$$Z_0^{\text{CPW}} = \frac{30\pi}{\sqrt{\epsilon_{\text{eff}}^{\text{CPW}}}} \frac{K(k)}{K(k')} \quad \Omega \tag{16}$$

where k and k' are given by (6). For a CPW on a substrate with a single dielectric layer, $\epsilon_{r1}^T = \epsilon_{r2}^T = \epsilon_{r3}^S = \epsilon_{r4}^S = 1$, and (14) becomes

$$\epsilon_{\text{eff}}^{\text{CPW}} = 1 + \frac{1}{2}(\epsilon_{r5}^S - 1)\frac{K(k)K(k_5')}{K(k')K(k_5)} \tag{17}$$

which is the equation given by Veyres and Fouad Hanna [13]. If the substrate can be considered as infinitely thick, i.e.,

$h_5 \to \infty$, then $k_5 = k$ and the effective dielectric constant is given as

$$\epsilon_{\text{eff}}^{\text{CPW}} = \frac{1}{2}(\epsilon_r + 1) \tag{18}$$

where ϵ_r is the dielectric constant of the substrate.

B. Wave Parameters of CPS's

The configuration of the CPS used for the analysis is shown in Fig. 1(b). Using Veyers–Fouad Hanna's approximation, the line capacitance of the CPS transmission line can be written as

$$C_{\text{CPS}} = C_0 + C_1 + C_2 + C_3 + C_4 + C_5. \tag{19}$$

Each capacitance has the same meaning as that of the CPW's except for the geometrical difference.

Line capacitance C_0, the capacitance when all the dielectrics do not exist, can be calculated using Schwartz transformations [23]. The result is given as

$$C_0 = \epsilon_0 \frac{K(k)}{K'(k)} \tag{20}$$

where

$$k = \sqrt{1 - \left(\frac{x_a}{x_b}\right)^2} \quad \text{and} \quad k' = \sqrt{1 - k^2} = \frac{x_a}{x_b}.$$

Although conformal mapping can also be used to calculate C_i $(i = 1, 2, 3, 4, 5)$, the obtained formulas, as pointed out by Ghione [14], give incorrect results, especially when the thickness of a dielectric layer is smaller than the dimensions of the transmission line's cross-section. However, under the quasi-static condition, the phase velocities of complementary lines are equal (Babinet's principle, see [24]). Noticing that a CPS is complementary with a CPW of which the ground wires are infinite wide, the effective dielectric constant of the CPS can then be obtained by taking $x_c \to \infty$ in (17), which gives

$$\begin{aligned}\epsilon_{\text{eff}}^{\text{CPS}} = 1 &+ \frac{1}{2}(\epsilon_{r1}^T - 1)\frac{K(k)K(k_1')}{K(k')K(k_1)} \\ &+ \frac{1}{2}(\epsilon_{r2}^T - \epsilon_{r1}^T)\frac{K(k)K(k_2')}{K(k')K(k_2)} \\ &+ \frac{1}{2}(\epsilon_{r3}^S - 1)\frac{K(k)K(k_3')}{K(k')K(k_3)} \\ &+ \frac{1}{2}(\epsilon_{r4}^S - \epsilon_{r3}^S)\frac{K(k)K(k_4')}{K(k')K(k_4)} \\ &+ \frac{1}{2}(\epsilon_{r5}^S - \epsilon_{r4}^S)\frac{K(k)K(k_5')}{K(k')K(k_5)}\end{aligned} \tag{21}$$

where

$$k_i = \sqrt{1 - \frac{\sinh^2\left(\frac{\pi x_a}{2h_i}\right)}{\sinh^2\left(\frac{\pi x_b}{2h_i}\right)}}, \qquad i = 1, 2, 3, 4, 5. \tag{22}$$

Using (1)–(3) and (20), we have

$$C_{\text{CPS}} = \epsilon_{\text{eff}}^{\text{CPS}} C_0 \tag{23}$$

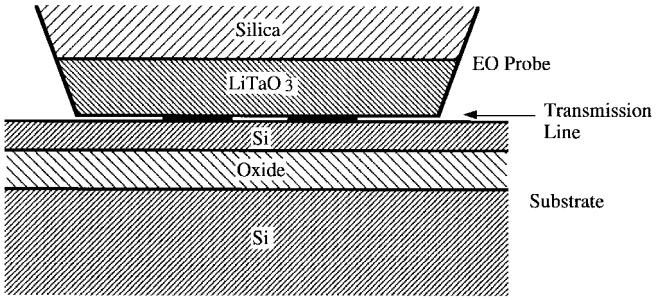

Fig. 3. Schematic diagram of the transmission line in the DEOS system.

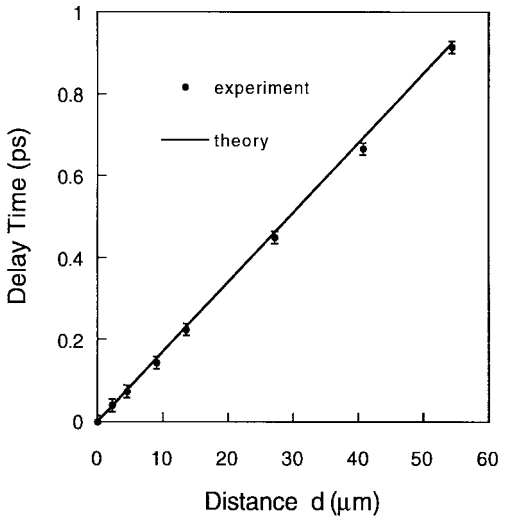

Fig. 4. Delay time versus propagation distance in the CPW on Si.

$$\nu_{\text{ph}}^{\text{CPS}} = \frac{c}{\sqrt{\epsilon_{\text{eff}}^{\text{CPS}}}} \tag{24}$$

$$Z_0^{\text{CPS}} = \frac{120\pi}{\sqrt{\epsilon_{\text{eff}}^{\text{CPS}}}} \frac{K(k')}{K(k)} \quad \Omega. \tag{25}$$

For a CPS on a single-layered substrate, $\epsilon_{r1}^T = \epsilon_{r2}^T = \epsilon_{r3}^S = \epsilon_{r4}^S = 1$, and the effective dielectric constant is

$$\epsilon_{\text{eff}}^{\text{CPS}} = 1 + \frac{1}{2}(\epsilon_{r5}^S - 1)\frac{K(k)K(k_5')}{K(k')K(k_5)} \tag{26}$$

which is Ghion's formula [14].

C. Simplification

The obtained formulas are given in the form of complete elliptical integrals of the first kind, which are difficult to calculate even with computers. They can be simplified using the approximations given by Hilberg [25], in which the ratio $K(k)/K'(k)$ is given as

$$\frac{K(k)}{K'(k)} \approx \frac{2}{\pi}\ln\left(2\sqrt{\frac{1+\text{k}}{1-\text{k}}}\right), \quad \text{for } 1 \le \frac{K}{K'} \le \infty \text{ and } \frac{1}{\sqrt{2}} \le k \le 1 \tag{27a}$$

TABLE I
PARAMETERS OF THE CPW AND CPS TRANSMISSION LINES

	CPW on Si	CPS on Si	CPS on SOI
$x_a(\mu m)$	6.75	5	5
$x_b(\mu m)$	17.25	24	24
$x_c(\mu m)$	117.25		
ε_{r1}^T	3.78	3.78	3.78
ε_{r2}^T	43	43	43
ε_{r3}^S	1	1	11.8
ε_{r4}^S	1	1	3.9
ε_{r5}^S	11.8	11.8	11.8
$h_1(mm)$	3.7	3.7	3.7
$h_2(\mu m)$	24	24	24
$h_3(\mu m)$			550
$h_4(\mu m)$			2.2
$h_5(nm)$	550	550	5
$v_{ph}^{exp}(\times 10^{10} cm/s)$	0.604	0.623	0.645
$v_{ph}(\times 10^{10} cm/s)$	0.588	0.597	0.609

$$\frac{K(k)}{K'(k)} \approx \frac{\pi}{2\ln\left(2\sqrt{\frac{1+k'}{1-k'}}\right)}, \quad \text{for } 0 \le \frac{K}{K'} \le 1 \text{ and } 0 \le k \le \frac{1}{\sqrt{2}}. \tag{27b}$$

The errors of these approximations are less than 0.3%. More accurate formulas can also be found in Hilberg's paper.

III. EXPERIMENT

A DEOS system has been used to measure the group velocities in CTL's on Si and SOI (Si-on-insulator) substrates. The setup of the system and its operation principle have been reported elsewhere [26]. What a DEOS system measures is the delay time in line section d of a transmission line, which is sandwiched by the substrate and the EO probe (Fig. 3). Therefore, there are two top dielectric layers (contributed by the EO probe) and one or three bottom dielectric layers (contributed by the substrates) involved in the measurements.

Delay times in three types of transmission lines were measured: 1) CPW's on Si; 2) CPS's on Si; and 3) CPS's on SOI. Transmission lines were fabricated using photolithography and liftoff. The widths of the ground and center wires of the CPW's were 100 and 13.5 μm respectively, spaced by 10.5 μm. The conducting wires of the CPS's were 19 μm wide, spaced by 10μm. All wires were made of 30/220-nm-thick Ti/Au metals. The Si substrate was from an n-type lightly doped Si wafer with a thickness of 550 μm. The 550-μm-thick SOI substrate was from a commercial wafer-bonded SOI wafer with a 2.2-μm-thick buried oxide (BOX) layer. The top Si layer (active layer) of the SOI substrate was thinned to 5–10-nm thick using thermal oxidation and high-frequency (HF) wet etch.

The DEOS system has an EO probe with a 24.0-μm-thick $LiTaO_3$ (dielectric constant $\epsilon_r = 43$) and a 3.7-mm-thick fused-silica base ($\epsilon_r = 3.78$). The effective area of the probe is 200×200 μm^2. The probe is in contact with the transmission line during the experiment, which has been ensured by checking the interference patterns generated between the surfaces of the probe and the transmission line. The rising time and full width at half-maximum of the electrical pulses generated by the pump beam were, respectively, 400 fs and 50 ps for the transmission lines on the Si substrate, and 400 fs and 10 ps for the transmission lines on the SOI substrate.

The DEOS system has a delay-time resolution of 30 fs and spatial resolution of 1 μm, which allows one to measure signal delays in a very short line length. Thus, the dispersion and absorption caused by the transmission line and the EO probe are minimized in the measurements, resulting in a very small pulse-shaping effect. The dispersion of the system has been found to be 0.3 fs/μm. Therefore, the variation in delay time caused by dispersion will be less than the time resolution of the system if the length of the measured transmission line is kept within 100 μm. Under this condition, the measured group velocity is close to the phase velocity in the transmission line. The absorption of the system has been measured to be 7% within a 200-μm line length.

IV. RESULTS AND DISCUSSION

Fig. 4 shows the measured delay times in the CPW on Si versus the signal propagating distances. The data show an excellent linearity indicating that it is close to the quasi-static value. The average group velocity calculated from the experimental data is 0.604×10^{10} cm/s. For comparison, the theoretical delay time calculated using (14) and (15) is

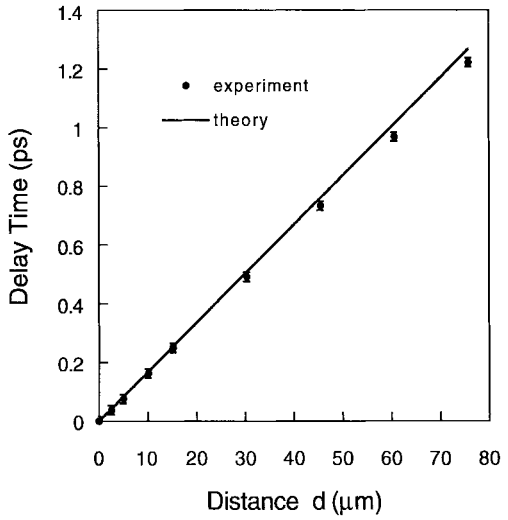

Fig. 5. Delay time versus propagation distance in the CPS on Si.

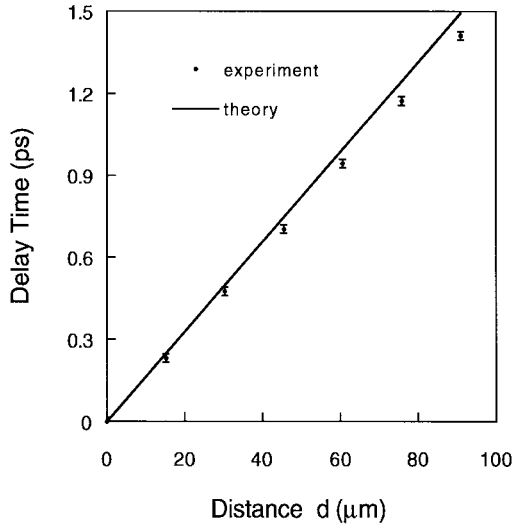

Fig. 6. Delay time versus propagation distance in the CPS on SOI.

also plotted in the figure. Parameters used for the calculation are listed in Table I. Since the thickness of the transmission line (0.25 μm) is much smaller than the line dimensions, it is ignored in the calculation. On the other hand, since the thicknesses of the bottom Si and fused-silica layers are much larger than the line dimensions, they have been considered to be infinite to facilitate the calculations. The theoretical group velocity is 0.588×10^{10} cm/s, differing from the experimental value by less than 3%. It should point out that, due to the loading effect of the EO probe, these velocities are about two times smaller than that when the EO does not exist [26].

Figs. 5 and 6 show, respectively, the measured delay times versus the signal propagating distances in the CPS's on the Si and SOI substrates. Excellent linearities have also been observed. The average group velocities calculated from the experimental data are 0.623×10^{10} and 0.645×10^{10} cm/s for the CPS's on the Si and SOI, respectively. Theoretical values calculated using (21) and (23) and parameters listed in Table I are also plotted in these figures. The theoretical group velocities are, respectively, 0.597×10^{10} and 0.609×10^{10} cm/s in the CPS's on the Si and SOI, with deviations from the experimental values less than 5% and 6%. Both the theory and experiment have indicated that the phase velocity of a transmission line on SOI is larger than that on Si. This is because the dielectric constant of the BOX in SOI is smaller than that of Si, which reduces the effective dielectric constant of the transmission line.

The deviation between the theory and experiment is slightly larger in the case of CPS than in CPW, presumably because more air exists inside the gap between the EO probe and the substrate of the CPS.

Fig. 7 shows the phase velocity of a CPS on an SiO_2/Si substrate as a function of the oxide thickness, calculated using (21) and (23). As the oxide thickness increases, the phase velocity also increases until the thickness of the oxide is comparable with the dimensions of the transmission line's cross section. At this point, the field only "sees" the oxide layer—the bottom Si layer has no contribution to the effective dielectric constant of the transmission line. For an oxide thickness of 2 μm, the phase velocity is about 10% larger than that without the oxide. When the oxide thickness increases to 100 μm, the increase in phase velocity reaches its maximum value of 58%.

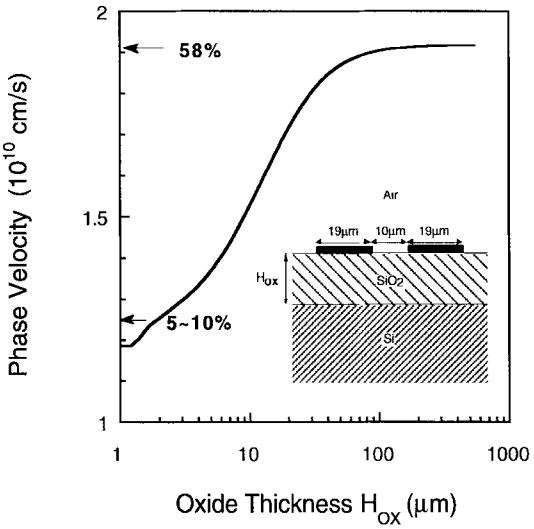

Fig. 7. Phase velocity as a function of the oxide thickness in a CPS line on a SiO_2/Si substrate. The inset is the structure of the transmission line used for the calculation.

V. Conclusions

We have obtained wave parameters of coplanar transmission lines expressed in analytical formulas using conformal mapping. The accuracy of these formulas is verified experimentally using differential EO sampling. For a CPW transmission line on an Si substrate, the theory differs from the experiment by less than 3%; for CPS transmission lines on Si and SOI substrates, the differences are less than 5% and 6%, respectively. Our calculation also shows that the phase velocity in a CPS on an SiO_2/Si substrate with oxide thickness of 2 μm is 10% larger than that on an Si substrate. This difference can increase to 58% if the oxide thickness becomes 100 μm.

REFERENCES

[1] P. Ho, M. Y. Kao, P. C. Chao, K. H. Duh, J. M. Ballingall, S. T. Allen, A. J. Tessmer, and P. M. Smith, "Extremely high gain 0.15 μm gate-length InAlAs/InGaAs/InP HEMT's," *Electron. Lett.*, vol. 27, pp. 325–327, 1991.

[2] D. A. Ahmari, M. T. Fresina, Q. J. Hartmann, D. W. Barlage, P. J. Mares, M. Feng, and G. E. Stillman, "High-speed InGaP/GaAs HBT's with a strained $In_xGa_{1-x}As$ base," *IEEE Electron Device Lett.*, vol. 17, pp. 226–228, 1996.

[3] D. M. Gill, B. C. Kane, P. Svensson, D.-W. Tu, P. N. Uppal, and N. E. Byer, "High-performance, 0.1 μm InAlAs/InGaAs high electron mobility transistors on GaAs," *IEEE Electron Device Lett.*, vol. 17, pp. 328–330, 1996.

[4] J. A. Valdmanis, "Electro-optic measurement techniques for picosecond materials, devices, and integrated circuits," in *Measurement of High-Speed Signals in Solid State Devices*, R. B. Marcus, Ed. San Diego, Ca: Academic, 1990, p. 136.

[5] M. Y. Frankel, J. F. Whitaker, and G. A. Mourou, "Optoelectronic transient characterization of ultrafast devices," *IEEE J. Quantum Electron.*, vol. 28, pp. 2313–2324, 1992.

[6] R. W. Jackson, "Consideration on the use of coplanar waveguide for millimeter-wave integrated circuits," *IEEE Trans. Microwave Theory Tech.*, vol. MTT-34, pp. 1450–1456, 1986.

[7] R. Majidi-Ahy, C. K. Nishimoto, M. Riaziat, M. Glenn, S. Silverman, S.-L. Weng, Y.-C. Pao, G. A. Zdasiuk, S. G. Bandy, and Z. C. H. Tan, "5–100 GHz InP coplanar waveguide MMIC distributed amplifier," *IEEE Trans. Microwave Theory Tech.*, vol. 38, pp. 1986–1993, 1990.

[8] M. Riaziat, R. Majidi-Ahy, and I.-J. Feng, "Propagation modes and dispersion characteristics of coplanar waveguides," *IEEE Trans. Microwave Theory Tech.*, vol. 38, pp. 245–251, 1990.

[9] K. C. Gupta, R. Garg, and I. J. Bahl, *Microstrip Lines and Slotlines.* Norwood, MA: Artech House, 1979.

[10] C. P. Wen, "Coplanar waveguide: A surface strip transmission line suitable for nonreciprocal gyromagnetic device applications," *IEEE Trans. Microwave Theory Tech.*, vol. MTT-17, pp. 1087–1090, 1969.

[11] M. E. Davis, E. W. Williams, and A. C. Celestini, "Finite-boundary corrections to the coplanar waveguide analysis," *IEEE Trans. Microwave Theory Tech.*, vol. MTT-21, pp. 594–596, 1973.

[12] P. A. J. Dupuis and C. K. Campbell, "Characteristics impedance of surface-strip coplanar waveguides," *Electron. Lett.*, vol. 9, pp. 354–355, 1973.

[13] C. Veyres and V. Fouad Hanna, "Extension of the application of conformal mapping techniques to coplanar lines with finite dimensions," *Int. J. Electron.*, vol. 48, pp. 47–56, 1980.

[14] G. Ghione and C. Naldi, "Analytical formulas for coplanar lines in hybrid and monolithic MIC's," *Electron. Lett.*, vol. 20, pp. 179–181, 1984.

[15] V. Fouad Hanna, "Finite boundary corrections to coplanar stripline analysis," *Electron. Lett.*, vol. 16, pp. 604–606, 1980.

[16] E. Yamashita and K. Atsuki, "Analysis of microstrip-like transmission lines by nonuniform discretization of integral equations," *IEEE Trans. Microwave Theory Tech.*, vol. 24, pp. 195–200, 1976.

[17] N. K. Das and D. M. Pozar, "A generalized spectral-domain Green's function for multilayer dielectric substrates with application to multilayer transmission lines," *IEEE Trans. Microwave Theory Tech.*, vol. 35, pp. 326–335, 197.

[18] M. Y. Frankel, R. H. Voelker, and J. N. Hilfiker, "Coplanar transmission lines on thin substrates for high-speed low-loss propagation," *IEEE Trans. Microwave Theory Tech.*, vol. 42, pp. 396–402, 1994.

[19] G. Hasnain, A. Dienes, and J. R. Whinnery, "Dispersion of picosecond pulses in coplanar transmission lines," *IEEE Trans. Microwave Theory Tech.*, vol. MTT-34, pp. 738–741, 1986.

[20] M. Y. Frankel, S. Gupta, and J. Valdmanis A., "Terahertz attenuation and dispersion characteristics of coplanar transmission lines," *IEEE Trans. Microwave Theory Tech.*, vol. 39, pp. 910–916, 1991.

[21] U. D. Keil, D. R. Dykaar, A. F. J. Levi, R. F. Kopf, L. N. Pfeiffer, S. B. Darack, and K. W. West, "High-speed coplanar transmission lines," *IEEE J. Quantum Electron.*, vol. 28, pp. 2333–2342, 1992.

[22] R. K. Hoffmann, *Handbook of Microwave Integrated Circuits.* Norwood, MA: Artech House, 1987.

[23] W. R. Smythe, *Static and Dynamic Electricity.* New York: McGraw-Hill, 1950.

[24] R. E. Collin, *Field Theory of Guided Waves.* New York: IEEE Press, 1991.

[25] W. Hilberg, "From approximations to exact relations for characteristic impedances," *IEEE Trans. Microwave Theory Tech.*, vol. MTT-17, pp. 259–265, 1969.

[26] E. Chen and S. Y. Chou, "Group velocities in coplanar strip transmission lines on Si and $Si/SiO_2/Si$ substrates measured using differential electro-optic sampling," *Appl. Phys. Lett.*, vol. 69, pp. 2861–2863, 1996.

Erli Chen received the B.S. degree in physics and the M.S. degree in optics from Beijing University, China, in 1982 and 1989, respectively. In 1992, he received the M.A. degree in solid-state physics from the State University of New York at Buffalo. He received the Ph.D. degree in electrical engineering from the University of Minnesota, Minneapolis, in 1997.

His research interests include nanofabrication and nonoscale electronic and optoelectronic devices.

Stephen Y. Chou (S'85–M'86–SM'92) received the Ph.D. degree from Massachusetts Institute of Technology, in 1986.

From 1986 to 1989, he was a Research Associate and then an Acting Assistant Professor in the Electrical Engineering Department, Stanford University, Stanford, CA. In 1989, he joined the University of Minnesota as an Assistant Professor, since 1994, he has been a Professor there. He has published over 150 journal and conference papers. His current research is in the areas of nanofabrication and nanoscale electronic, optoelectronic, and magnetic devices.

Dr. Chou has received the Packard Fellowship, McKnight–Land Grant Professorship, IBM Faculty Development Award, and George Taylor Distinguished Research Award.